NAZARBAYEV UNIVERSITY

Bachelor of Engineering

(Mechanical)

Hemodynamic Design Optimization of a Blood-wetted Medical Device associated to treatment of Cardiovascular Diseases applying Computational Fluid Dynamics:

Case study of Kazakhstan

(Final Capstone Project Report)

By

Nurassyl Kussaiyn

Yertay Mendygarin

Principal Supervisor: Luis Rojas-Solórzano

April, 2017

DECLARATION

We hereby declare that this report entitled "Hemodynamic Design Optimization of a Blood-wetted Medical Device associated to treatment of Cardiovascular Diseases applying Computational Fluid Dynamics: Case study of Kazakhstan" is the result of our own project work except for quotations and citations which have been duly acknowledged. We also declare that it has not been previously or concurrently submitted for any other degree at Nazarbayev University

---

Name: Yertay Mendygarin
Date:

Name: Nurassyl Kussaiyn
Date:

Acknowledgements

We would like to express our deepest appreciation to all those who provided us the possibility to complete the first part of the Capstone Project. A special gratitude we give to our capstone project supervisor, Luis Rojas, whose contribution in stimulating suggestions and encouragement helped us to coordinate our project and National Scientific Research Center in Astana for their cooperation with our team. Also, we want to thank Nazarbayev University for the support of this investigation through the Research Seed Grant № КФ -14/11.

Abstract

This project aims to the improvement and validation of a multiphase fluid dynamics numerical model of blood flow to provide more accurate modeling of blood damage occurring within blood-wetted medical devices. Heart diseases are responsible for a significant portion of deaths worldwide and particularly in Kazakhstan, where blood-wetted medical devices are increasing in their use as a vital tool in the treatment of these diseases, supporting patient's lives or as a bridge to needed transplants. However, these devices can introduce problems associated with biocompatibility of the materials or due to prolonged large shear stresses acting on blood cells. Within the family of blood-wetted devices used for cardiovascular diseases, the Ventricular Assist Devices (VAD) are of profound consideration, especially nowadays in Kazakhstan. Computational Fluid Dynamics (CFD) is proven to be a very useful and promising tool to perform blood flow simulations, as it is less expensive and time-saving compared with in-vitro experiments with real blood. Nevertheless, there is still lack of agreement between scientists worldwide about accurate modeling blood damage using CFD tools. This project aims to recover a current state-of-the-art multiphase CFD model of blood and tackle some of its potential weaknesses to improve its predictability characteristics. In particular, an Eulerian-Eulerian multiphase model, developed by the advisor of this investigation and his graduate student team, with moderate accuracy on prediction of blood damage, will be subject to modifications to include a new sub-model based on the principles of Granular Kinetic Theory (GKT) aiming to a better capture of blood cells segregation, which is blamed as the main cause of inaccuracies of that model. The existing model improved the blood damage prediction from a predecessor homogeneous model by just incorporating a particle-like nature to red blood cells (RBC) and platelets (PLT) transported in the blood stream. However, at the beginning of this investigation there was still large space to improve the damage prediction. The major inaccuracy of the base model was hypothesized as its incapability of predicting the correct peak of concentration of platelets that is expected to occur very near the vessel wall, also called the Fahraeus-Lindqvist (F-L) effect. Indeed the base model designed to simulate a three-phase plasma-RBC-PLT fluid flow, considering interfacial interaction between PLT and RBC only with plasma in a single-particle-interaction approach, was capable to predict a peak of platelet concentration near the wall, but with intensity much lower than expected. Therefore, the GKT sub-model incorporated

in this investigation was expected to capture a more realistic cell-cell interaction, cell-wall and cell-plasma interaction such that the prediction of the F-L effect is improved and thus, a better damage modeling might be obtained in the next stage of the calculation. Therefore, the model proposed in this investigation improves it's the base model by taking into account not only interactions between disperse and continuum phases, but also the interactions among the disperse phases with the use of the GKT. Earlier deliverables of the project included damage model for blood flow and optimization of the cannula tip shape of VAD using the base model in order to understand its limitation and scope.

During the realization of this project, initially an ambitious goal expected to conclude with the improvement, validation, incorporation of damage and optimization of the same cannula as before, but the time-constraints and complexity of the problem made us to re-dimension the scope to the improvement of the F-L effect as a mean to grant a better base model to further predict later blood damage and subsequent optimization of the cannula or other blood-wetted devices. Therefore, several simulation parameters were chosen for in-depth analysis on how the F-L effect is predicted under variation of parameters that affect the particles (cells) segregation within the flow.

Table of contents

List of figures

List of tables

List of abbreviations:

d – pipe diameter

d_p– diameter of particle

e – restitution coefficient

$\vec{g}$ – gravitational acceleration

g_o – radial distribution function

$\vec{\vec{I}}$ – unit tensor

k – granular conductivity

k_r – Extinction coefficient of the absorbing medium for RBC

k_s – Extinction coefficient of the absorbing medium for platelet

∇P – pressure gradient

∇P_f – pressure gradient for plasma

∇P_r – pressure gradient for RBC

∇P_s – pressure gradient for platelet

$\vec{v}_f$ – plasma phase velocity vector

$\vec{v}_r$ – RBC phase velocity vector

$\vec{v}_s$ – platelet phase velocity vector

Greek letters

β – drag coefficient between particles

ρ_s – platlet phase density

ρ_f – plasma phase density

ρ_r – RBC phase density

ε_f – volume fraction of plasma

ε_r – volume fraction of RBC

ε_s – volume fraction of platelet

$\varepsilon_{s,max}$ – maximum platelets volume fraction

τ – shear stress

$\vec{\vec{\tau}}_f$ – stress tensor of plasma

$\vec{\vec{\tau}}_r$ – stress tensor of RBC

$\vec{\vec{\tau}}_s$ – stress tensor of platelets

$\nabla \cdot \vec{\vec{\tau}}_f$ – Divergence of the stress tensor of the plasma

$\nabla \cdot \vec{\vec{\tau}}_r$ – Divergence of the stress tensor of RBC

$\nabla \cdot \vec{\vec{\tau}}_s$ – Divergence of the stress tensor of platelet

θ – Granular temperature

γ – Energy dissipation due to inelastic collision of particles

μ_f – plasma viscosity

μ_r – RBC viscosity

μ_s – platelet viscosity

ξ_f – bulk viscosity of plasma

ξ_r – bulk viscosity of RBC

ξ_s – bulk viscosity of platelets

1. Introduction

The main aim of this capstone project is to propose and validate an improved numerical multiphase model of blood flow intended to be used to predict blood damage through blood-wetted medical devices. These devices are widely used in treatment of cardiovascular diseases as they help to provide better blood flow for patients with severe cardiovascular diseases for bridging-to-transplant and/or destination therapy. As the blood flows through non-biological walls of pipes, connectors, vessels, containers and complex devices, "blood damage" may occur. This damage emerges due to lack of biocompatibility or due to excessive shear stresses acting during prolonged periods of time which can disrupt the membrane of red blood cells leading to hemolysis as well as thrombus formation due to activation of platelets. As the blood damage can be very harmful for the patient's health, proper designs of such devices are required. Nevertheless, in-vitro experiments with blood can be expensive and potentially raise ethical issues and therefore, simulation of blood behavior using Computer Fluid Dynamics has emerged as an inexpensive and potentially accurate tool appropriate for these studies. Thus, optimization of blood-wetted devices using Computational Fluid Dynamics would be highly desired, but current limitations on accuracy of multiphase modeling and ulterior damage are still a lesson to be learned and completed by the world scientific community. The attempt of the present study is to improve current multiphase model of blood flow to the extent of predicting more accurately the distribution of blood cells through the flow stream. We believe that current limitations of the blood damage model lie on the lack of accurate prediction of location of blood cells and therefore, for example, prediction of red blood cell damage in regions where these cells are inexistent or in lower concentrations. Developing a better multiphase model with improved accuracy of cells concentration will allow the ulterior prediction of blood damage (i.e., hemolysis and platelets lysis in this case) and provide the needed computational tool for optimization purposes that is currently lacking in the community.

It is important to mention that Ventricular Assist Devices and many other blood-wetted elements are currently in extensive use in Kazakhstan, where the mortality per capita due to cardiovascular disease is the 5^{th} in the world (WHO, 2011). Therefore, this project has a fundamental relevance in cardiovascular, CFD-scientific and in many countries in the world, as Kazakhstan, for which VAD and other blood-wetted medical equipment are expected to keep in the rise.

Our simulations of blood flow were based on finite volume method using existing Eulerian-Eulerian multiphase (liquid-particles). The main contribution of our work is the use of a closure model for the solid phase (particles modeling blood cells) based on Granular Kinetic Theory (GKT). GKT has proven in previous works, modeling slurry flows, to be a good model to predict particle concentration and pressure drop by taking into account the contribution of collisional, kinetic and frictional contributions to the stress tensor of the segregated solid phase. The key point of this study is that it takes into account not only interactions between disperse and continuum phases, but also the interactions among the disperse phases with the use of the GKT, under the assumption that each phase is present in each control volume and has a volume fraction equal to the fraction of the control volume occupied by that phase.

The results of the project are expected to provide a much better multiphase numerical platform to be used in future modeling of blood damage.

2. Background

Cardiovascular Disease (CVD), commonly referred as Heart Disease, involves the heart and blood vessels (arteries, veins and capillaries) (Maton et al., 1993) associated to the cardiovascular system, i.e., cardiac, brain, kidney, vascular and peripheral artery systems. These diseases are killing more and more people around the world, striking rich and poor alike (Kulkayeva et al., 2012) and contributing significantly to the health costs in both developed and developing countries.

Kazakhstan suffers from one of the highest cardiovascular mortality rates in the world. According to the World Health Organization (2010) data, age-standardized CVD mortality rates in Kazakhstan were 650 per 100,000 inhabitants in 2008. CVD mortality among men is especially high (the age-standardized CVD mortality rates among men were 859 per 100,000), while among women this number was one and half times less, 549 per 100,000 inhabitants (Davletov K. et al, 2015). Premature mortality because of CVD took second place in all countries of the Commonwealth of Independent States, and was 3–4 times higher in Kazakhstan than in Western European countries (Kulkayeva et al., 2012). Continued morbidity, mortality and disability of people suffering from CVD, especially among the working population, greatly harms economic development and represents a high burden to society. CVD persists as a main

killer, particularly among middle-aged males throughout Europe and in Kazakhstan (Kulkayeva et al., 2012). The author states that, in 2005, more than 30.0% of Kazakh people who died from CVD were of working age (20–65 years), and almost 70.0% were males. These results demonstrate that CVD can affect to the economy of the whole country.

In the treatment of CVD-related pathologies, sometimes surgical remedies are used, in which heart of the patients must be stopped and artificial assistance needs to be applied during the intervention process.

When blood is in contact with a non-biological environment, many complications may take place. Thermal and osmotic effects and even the contact with the walls of artificial vessels may cause damage to the blood cells due to lack of biocompatibility. Nevertheless, the most relevant type of damage is caused by the abnormal exposition of the cells to shear stresses for a prolonged period of time (Salazar et al., 2008). Above critical conditions of shear stress and time of exposition, these stresses may cause the rupture or partial damage of the membrane that covers the red blood cells, allowing the release of hemoglobin into the plasma in a process known as hemolysis (Fig 1.)

Figure 1: Hemolysis (source: http://pnhahus.com.au/pnh/)

However, shear stresses do not only affect the red blood cells, but also may affect platelets, changing their fibrinogen receptors and increasing the possibility to generate some aggregates and making the platelets more likely to stick to the surface of the blood vessels and get activated creating thromboses, with catastrophic consequences for the patient (Tandon and Diamond, 1997).

In order to validate the performance of the blood-wetted devices numerous in-vitro testings with human or animal blood are necessary. As these experiments are associated with high costs and time, and moreover can raise ethical issues, simulation of blood behavior using Computer Fluid Dynamics can be inexpensive and appropriate for testing. Therefore,

optimization of blood-wetted devices using CFD was chosen as the inexpensive and consistent solution. However, there is still huge discrepancy between the methods proposed by scientists and the results obtained still are not accurate enough to validate the performance of high-precision VADs.

In 2007 Food and Drug Administration (FDA) of the USA announced a call for the project called "Critical Path Initiative" aiming to standardize and reduce discrepancies between CFD models for flow fields prediction and blood damage by 2010 (Stewart et al., 2009). Over 28 groups from all over the world produced studies on a flow model to determine the best method for CFD results extrapolation to predict blood damage potential of medical devices. Nevertheless, preliminary results presented in 2009 concluded that there was still lack of agreement among different methods used by groups. Therefore, the need for more accurate models for blood damage prediction is still relevant in the scientific community.

2.1 Literature review on the blood rheology and hemolysis

Early attempts to calculate blood hemolysis failed to emulate real blood damage values found during in vitro experiments. The reason for this was that although blood at macroscopic level is considered as homogeneous, at microscopic level it consists of different cells. Therefore, to accurately predict level of blood damage, blood was considered as a multiphase flow composed by plasma, RBC and platelets (Mubita et al. 2014). In a recent study of Mubita et al. (2015), authors attempted to create a multiphase model to reduce the existing gap between experimental and simulated values of hemolysis. In their numerical tests, the model was tuned up to capture the non-uniform distribution of blood cells and the damage differential equation based on correlation proposed by Giersiepen et al. (1990) was applied to RBC phase only. Mubita et al. (2015) demonstrated that hemolysis level obtained by multiphase flow is much closer to experimental values rather than homogeneous flow model. Nevertheless, authors acknowledged that although the model captures the segregation of platelets, it under-predicts the peak concentration of these particles near the wall, thus overestimating the number of RBC and the ulterior predicted RBC damage near the wall where the shear stress are expected to be higher.

In another study, Zhao et al. (2008) studied a suspension of RBCs and platelet-sized fluorescent polystyrene particles at controlled flow rates (6–30 $mL \times h^{-1}$) through a micro-channel

containing a 100–200 μm expansion. The primary aim of this study was to elucidate the thrombogenicity of microscopic flow by determining how the local platelet concentration is affected by changing the hematocrit level of blood within physiological range in the flow separation of a region of sudden expansion. The results proved the strong influence of hematocrit level on platelets near-wall concentration in the region of sudden expansion of connectors. Zhao et al. (2008) concluded that to properly simulate the platelets transport and thus predict formation of thromboses, multiphase flow modeling should be used to account for RBC's and platelets interaction.

To account for the spatial distribution of the blood elements within the flow, number of researcher have conducted numerical simulations. Gidaspow and Huang (2009) applied Granular Kinetic Theory-based two-phase flow model to explain Fahraeus–Lindqvist effect, which corresponds to the migration of red blood cells from the wall to the center in narrow tubes. Tandon et al. (2015) also studied the migration of RBC from wall to center, and performed modeling using two different approaches: one base on Granular Kinetic Theory and the second, two-fluid theory based suspension rheology. According to GKT, the migration of RBC is caused by decrease of granular temperature, the random kinetic energy for red blood cells per unit mass, at the center of the tube due to inelastic collisions. As this granular temperature is the driving force for migration, the magnitude of inelasticity is the only significant empirical parameter in this model. Gidaspow and Huang (2009) concluded that hematocrit level computed with kinetic theory model agree with experimental measurements. Tandon et al. (2015) also concluded that for both GKT and Suspension model, the numerical simulation results agree with experimental values, although the GKT approach predicts near wall hematocrit concentrations better because it accounts for inelasticity of the walls. Nevertheless, Mubita et al. (2014) pointed out that although this model estimates RBC concentration fairly well, in their model, previous authors ignored the presence of platelets.

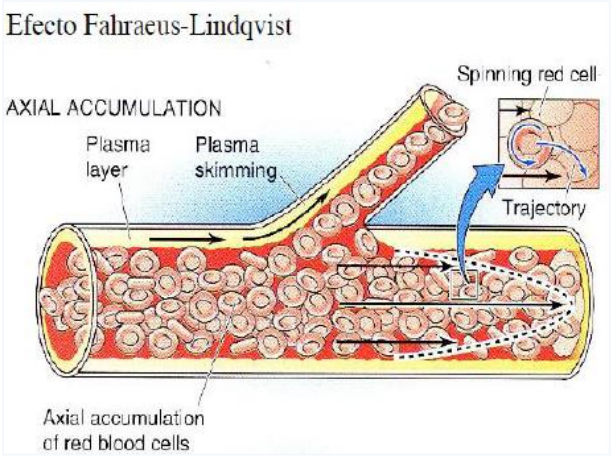

Figure 2. Fahraeus–Lindqvist effect (source: Eckstein & Belgacem, 1991)

2.2 Overview on VAD's

A ventricular assist device is a pump that is attached between the heart and the aorta or pulmonary artery which helps to circulate a person's blood when the heart can no longer adequately support circulation. The aim of such a device is to unload the heart and to provide an adequate peripheral circulation with sufficient organ function. In reducing cardiac work and oxygen consumption the required energy for repair processes and synchronized heart performance can be spared and leads to a quicker recovery of "stunned" myocardial segments (Waldenberger, 1997).

In Kazakhstan, due to the geographical and cultural reasons, the lack of qualified specialists does not favor the development of heart transplant procedure. Therefore, a special surgical program for treatment of advanced refractory heart failure was implemented, focusing main efforts on VAD therapy. The program upheld and financed by the national healthcare system, is based on a single, highly specialized surgical Center for the operation, and on a regional infrastructure for outpatient follow-up. Local VAD coordinators are taught by the National Center. They are accountable for standard patient check, anticoagulant and antiplatelet treatment prescription and continuing patients' and caregivers' education (Davletov et al, 2015).

From November 2011 to November 2014, 146 patients underwent implantation of 152 VADs at National Research Cardiac Surgery Center (approximately 50 devices implanted per year). Excluding HeartMate III devices, 138 patients were implanted with 144 VADs. A total of

135 patients received a device for left ventricular assist, and of these, 95 patients (65%) received a HeartMate II device and 40 patients (26%) received a HeartWare device for left ventricular assist. Two patients received BiVADs, and one received total artificial heart using two pumps. Three patients underwent pre-implantation of original LVAD because of pump thrombosis (Pya et al, 2016).

The existence of the VAD program is now stimulating the growth of heart transplantation in Kazakhstan. From the given data above, HeartMate III device was one of the most popular blood-wetted devices used in Kazakhstan medicine. Within the framework of capstone program, our group visited the National Scientific Research Center and verified in wide usage of HeartMate III device.

3. Methodology

The model used in this project simulates blood as a multiphase fluid flow using an Eulerian-Eulerian approach based on the model used for simulations of liquid-solid slurry For granular flows, there are three flow regimes: an elastic regime, a plastic regime and a viscous regime. The elastic regime is stagnant and the stress is strain dependent. Elasticity can be used to model the motion. The plastic regime is similar to viscous regime but the flow is still slow and the strain rate is independent of the stress. The viscous regime can be characterized with rapid flow. This flow regime is strain rate dependent and the motion of the granular phase can be modeled by applying kinetic theory (Gonzalez, 2012).

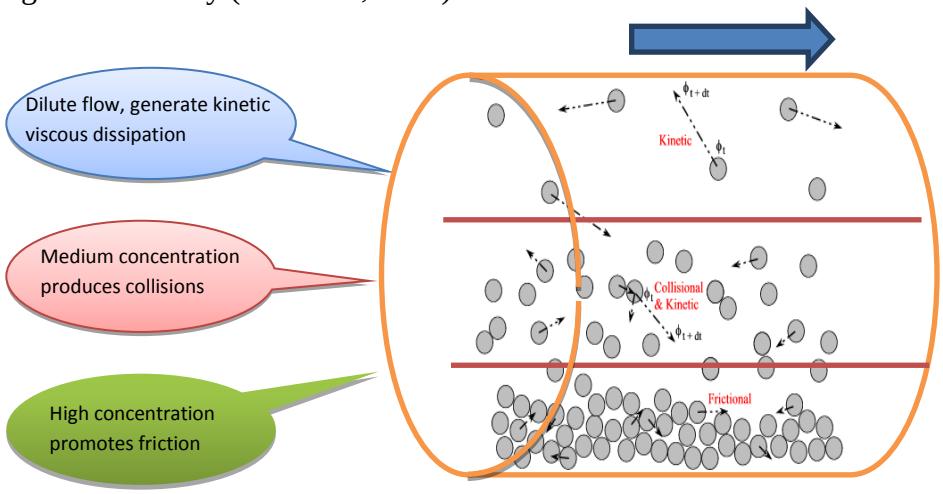

Figure 3. Heterogeneous-saltation regimes in Solid-liquid flow (source: Gonzalez, 2012)

Blood's flow behavior in small vessels behaves as Non-Newtonian fluid. Fahraeus and Lindqvist (1931) have founded that blood viscosity depends on the vessel diameter. Since the discovery of F-L effect, different in vitro studies were done which confirmed this effect. It was expected that red blood cells (RBCs) move from the wall to the center in small vessels and near the wall forms cell-free layer reducing blood viscosity. This nature of multiphase fluid explains the physical reason of Fahraeus–Lindqvist effect.

Viscosity of red blood cells in this kinetic theory model computed using random kinetic energy equation, called granular temperature. Gidaspow et al. (2009) reviewed the kinetic theory of granular flow created by Savage and others, explaining particles movement. Random oscillations of particles produced by wall-shear cause this granular temperature to rise near the wall. The granular temperature is the driving force for particle migration, like thermal diffusion in gases. However, in flow of heavy particles in liquids, particle move toward the wall and form a core-annual flow in vertical pipes as suspended particles in gases.

In this paper, the blood viscosity is not an empirical input into the model. It is computed from the theoretical expressions obtained from the kinetic theory of granular flow. Experiments show that the particulate viscosity expression obtained from the kinetic theory gives the same results as that measured by classical methods. The basic mass and momentum balances for the plasma and the red blood cells are as follows (f = plasma, r = RBCs, s = platelets).

Plasma mass balance:

$$\frac{\partial(\rho_f \varepsilon_\mathrm{f})}{\partial t} + \nabla \bullet \left(\rho_f \varepsilon_\mathrm{f} \overrightarrow{\mathrm{v_f}}\right) = 0 \tag{1}$$

RBC mass balance:

$$\frac{\partial(\rho_r \varepsilon_\mathrm{r})}{\partial t} + \nabla \bullet (\rho_r \varepsilon_\mathrm{r} \overrightarrow{\mathrm{v_r}}) = 0 \tag{2}$$

Platelets mass balance:

$$\frac{\partial(\rho_s \varepsilon_\mathrm{s})}{\partial t} + \nabla \bullet (\rho_s \varepsilon_\mathrm{s} \overrightarrow{\mathrm{v_s}}) = 0 \tag{3}$$

where ε is a volume fraction, ρ is density, t is time, $\vec{v}$ isvelocity vector with the subscript indicating the phase.

Plasma momentum balance:

$$\frac{\partial(\rho_f \varepsilon_f \vec{v}_f)}{\partial t} + \nabla \cdot \left(\rho_f \varepsilon_f \overrightarrow{v_f} \overrightarrow{v_f}\right) = \rho_f \varepsilon_f \vec{g} - \varepsilon_f \nabla P + \nabla \cdot \vec{\tau}_f + \beta(\vec{v}_s + \overrightarrow{v_r} - \vec{v}_f) \quad (4)$$

RBC momentum balance:

$$\frac{\partial(\rho_r \varepsilon_r \vec{v}_r)}{\partial t} + \nabla \cdot (\rho_r \varepsilon_r \overrightarrow{v_r} \overrightarrow{v_r}) = \rho_r \varepsilon_r \vec{g} - \varepsilon_r \nabla P - \nabla P_r + \nabla \cdot \vec{\tau}_r + \beta(\vec{v}_f + \overrightarrow{v_s} - \overrightarrow{v_r}) \quad (5)$$

Platelet momentum balance:

$$\frac{\partial(\rho_s \varepsilon_s \vec{v}_s)}{\partial t} + \nabla \cdot (\rho_s \varepsilon_s \overrightarrow{v_s} \overrightarrow{v_s}) = \rho_s \varepsilon_s \vec{g} - \varepsilon_s \nabla P - \nabla P_s + \nabla \cdot \vec{\tau}_f + \beta(\vec{v}_f + \overrightarrow{v_r} - \overrightarrow{v_s}) \quad (6)$$

where P is fluid pressure, P_s is granular pressure, P is fluid pressure, $\vec{g}$ is gravity acceleration, $\vec{\tau}_r$ is stress tensor, and β is the interface momentum exchange coefficient.

The sum of each phase volume fractions should to be one:

$$\varepsilon_f + \varepsilon_r + \varepsilon_s = 1 \quad (7)$$

The random kinetic energy equation for RBCs and platelets are expressed as:

$$\frac{3}{2}\left[\frac{\partial(\rho_r \varepsilon_r \theta)}{\partial t} + \nabla \cdot (\rho_r \varepsilon_r \theta \overrightarrow{v_r})\right] = \left(-P_r \vec{\vec{I}} + \vec{\vec{\tau}}_r\right) : \nabla \vec{v}_r + \nabla \cdot (k_r \nabla \theta) - \gamma \quad (8)$$

$$\frac{3}{2}\left[\frac{\partial(\rho_s \varepsilon_s \theta)}{\partial t} + \nabla \cdot (\rho_s \varepsilon_s \theta \overrightarrow{v_s})\right] = \left(-P_s \vec{\vec{I}} + \vec{\vec{\tau}}_s\right) : \nabla \vec{v}_s + \nabla \cdot (k_s \nabla \theta) - \gamma \quad (9)$$

Accumulation + Net outflow = Production + Conduction – Dissipation

where θ is granular temperature which is defined as the mean of the squares of particle velocity fluctuation, k is granular conductivity, and γ is the collisional energy dissipation. The granular temperature is a measure of the random particle kinetic energy per unit mass. It is produced due to "viscous type dissipation" and consumed due to inelastic collisions.

The stress tensor for each phase is given by a Newtonian type viscous approximation, as:

$$\vec{\vec{\tau}}_f = \varepsilon_f \mu_f \left(\nabla \vec{v}_f + \nabla \overrightarrow{v^T}_f\right) - \frac{2}{3} \varepsilon_f \mu_f \nabla \cdot \vec{v}_f \vec{\vec{I}} \quad (10)$$

$$\vec{\vec{\tau}}_r = \mu_r\left(\nabla\vec{v}_r + \nabla\overrightarrow{v^T}_r\right) + (\xi_r - \frac{2}{3}\mu_r)\nabla\cdot\vec{v}_r\vec{\vec{I}} \tag{11}$$

$$\vec{\vec{\tau}}_s = \mu_s\left(\nabla\vec{v}_s + \nabla\overrightarrow{v^T}_s\right) + (\xi_s - \frac{2}{3}\mu_s)\nabla\cdot\vec{v}_s\vec{\vec{I}} \tag{12}$$

RBC pressure, P_s, shear viscosity, μ_s, and bulk viscosity, ξ_s, are expressed as a function of granular temperature based on the kinetic theory model.

$$P_r = \rho_r\varepsilon_r\theta + 2\rho_r(1+e)\varepsilon^2{}_r g_0\theta \tag{13}$$

$$\mu_r = \frac{4}{5}\varepsilon^2{}_r\rho_e d_p g_0(1+e)\left(\frac{\theta}{\pi}\right)^{1/2} + \frac{10\rho_r d_p\varepsilon_r\sqrt{\theta\pi}}{96(1+e)g_0}[1+\frac{4}{5}\varepsilon_r g_0(1+e)]^2 \tag{14}$$

$$\xi_r = \frac{4}{3}\varepsilon^2{}_r\rho_r d_p g_0(1+e)\left(\frac{\theta}{\pi}\right)^{1/2} \tag{15}$$

For platelets:

$$P_s = \rho_s\varepsilon_s\theta + 2\rho_s(1+e)\varepsilon^2{}_s g_0\theta \tag{16}$$

$$\mu_s = \frac{4}{5}\varepsilon^2{}_s\rho_s d_p g_0(1+e)\left(\frac{\theta}{\pi}\right)^{1/2} + \frac{10\rho_s d_p\varepsilon_s\sqrt{\theta\pi}}{96(1+e)g_0}[1+\frac{4}{5}\varepsilon_s g_0(1+e)]^2 \tag{17}$$

$$\xi_s = \frac{4}{3}\varepsilon^2{}_s\rho_s d_p g_0(1+e)\left(\frac{\theta}{\pi}\right)^{1/2} \tag{18}$$

where d_p is the diameter of the particle, g_0 is the radial distribution function, and *e* is the restitution coefficient, which is a measure of the elasticity of the particle-particle collision. It is defined as the ratio of rebound velocity of particle to its velocity before impact.

The radial distribution function expressing the statistics of the spatial arrangement of the particles is given by a geometric approximation, the Bagnold's equation, as:

$$g_0 = [1 - (\frac{\varepsilon_s}{\varepsilon_{s,max}})^{1/3}]^{-1} \tag{19}$$

$$g_0 = [1 - (\frac{\varepsilon_r}{\varepsilon_{r,max}})^{1/3}]^{-1} \tag{20}$$

The granular conductivity, k_s, consists of the kinetic part from dilute kinetic theory of gases and the collisional part due to inelastic collision of particles, as reviewed by Gidaspow.

$$k_s = \frac{150\rho_s d_p \varepsilon_s \sqrt{\theta\pi}}{384(1+e)g_0}[1+\frac{6}{5}\varepsilon_s g_0(1+e)]^2 + 2\varepsilon^2{}_s \rho_s d_p g_0(1+e)\left(\frac{\theta}{\pi}\right)^{1/2} \quad (21)$$

$$k_r = \frac{150\rho_r d_p \varepsilon_r \sqrt{\theta\pi}}{384(1+e)g_0}[1+\frac{6}{5}\varepsilon_r g_0(1+e)]^2 + 2\varepsilon^2{}_r \rho_r d_p g_0(1+e)\left(\frac{\theta}{\pi}\right)^{1/2} \quad (22)$$

The energy dissipation due to inelastic collision of particles, first evaluated by Savage and his colleagues, is given by:

$$\gamma = \frac{12(1-e^2)g_0}{d_p\sqrt{\pi}}\varepsilon^2{}_s \rho_s \theta^{3/2} \quad (23)$$

$$\gamma = \frac{12(1-e^2)g_0}{d_p\sqrt{\pi}}\varepsilon^2{}_r \rho_r \theta^{3/2} \quad (24)$$

4. Implementation chapter

4.1.Physical Properties and Numerical Set-up

Eulerian–Eulerian multiphase model was used for the experiment in a narrow tube by Yeh et al. (1994) to obtain numerical simulation results. Blood was considered as a multiphase fluid containing plasma, RBCs, and PLTs. The plasma phase was modeled as a continuous Newtonian fluid with a viscosity of 0.0012 Pa×s and a density of 1,025 kg×m^{-3}. RBCs and PLTs were modeled as a spherical particle-like fluid dispersed with a density of 1,100 and 1,040 kg×m^{-3}, respectively. Sauter mean diameters of 6 μm for RBCs and 2.5 μm for PLTs were assumed. In this investigation, the viscosity of the disperse phases was not an empirical input into the model; it was computed from the theoretical expressions obtained from the kinetic theory of granular flow.

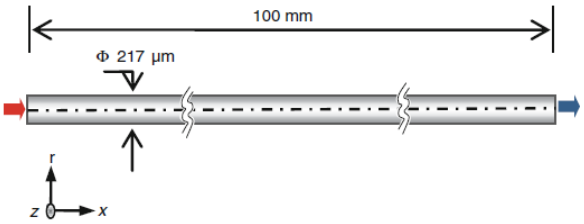

Figure 4. Computational domain tube (source: Yeh et al., 1994)

Figure 4 shows a scheme of the computational domain tube with constant cross-section. The length of the tube is 100 mm and the internal diameter is 217 µm equivalent to ~35 times the mean Sauter diameter of RBCs and the geometry is depicted by assuming axis-symmetry. During the simulation, whole tube was considered full of uniform mixture of plasma, RBC and platelets, with volume fractions (α) of 58, 40, and 2% respectively, granular temperature for disperse phases was 1×10^{-8} $m^2\times s^{-2}$. The inlet flow is set such that the axial velocities had similar values equivalent to Poiseuille average wall shear rate (555 s^{-1}) used by Yeh et al. (1994). Thus, all phases are set to have 1.505×10^{-2} $m\times s^{-1}$ axial velocity and zero value for radial velocity. Exit of the domain had free-stress condition, while in the wall considered zero velocity/no-slip condition. Turbulence effects were not performed, because of low Reynolds number (Re<5) (Mubita et al., 2014). Flow parameters can be reviewed on Table 1.

Phase	**Plasma**	**RBC**	**Platelet**
Density [kg×m^{-3}]	1,025	1,100	1,040
Viscosity [kg×m^{-1}s^{-1}]	0.0012	to be calculated	to be calculated
D_p [µm]	---	6	2.5
Volume Concentration [%]	58	40	2
Velocity [m×s^{-1}]	1.505×10^{-2}	1.505×10^{-2}	1.505×10^{-2}

Table 1. Flow properties (source: Yeh et al., 1994)

The convergence and normalized errors accepted in the simulations were in the order of 10^{-8} for the equations of momentum, turbulence, volumetric fraction and granular temperature. The difference in total mass flow between the inlet and outlet did not exceed 2.05×10^{-3} % for all runs. QUICK scheme was applied for the discretization spatial distribution of the convective term. The mathematical model was created in ANSYS Fluent v.17.2, where the residuals were

monitored and the granular temperature, restitution coefficient, drag coefficient and packing limit of the GKT model were adjusted to determine their effects on final result.

4.2. Verification of Grid Independence

A study of grid convergence was undertaken to confirm the solution's independence from grid resolution. The conducted procedure reduced the truncation error and found best degree of grid resolution. The method consists in starting with an initial grid and then making consecutive refinements to observe the effect of the grid. Grid Convergence Index based on the Richardson Extrapolation method was used for discretization error estimation (Mubita et al., 2014). This method compares three different grid sizes. Three structured and stepped grids (coarse, medium and fine) with hexaedrical elements were prepared by using ANSYS FLUENT MESH. The finite elements mesh carefully modeled near the wall region. Table 2 shows the number of computational cells for each one of the generated meshes. The refinement factors $r_{21}=h_{medium}/h_{fine}$ and $r_{32}=h_{coarse}/h_{medium}$ were 1.4 in all cases.

Mesh	**Elements**
Coarse	201810
Medium	309876
Fine	488250

Table 2. Uniform structured grids with total number of cells

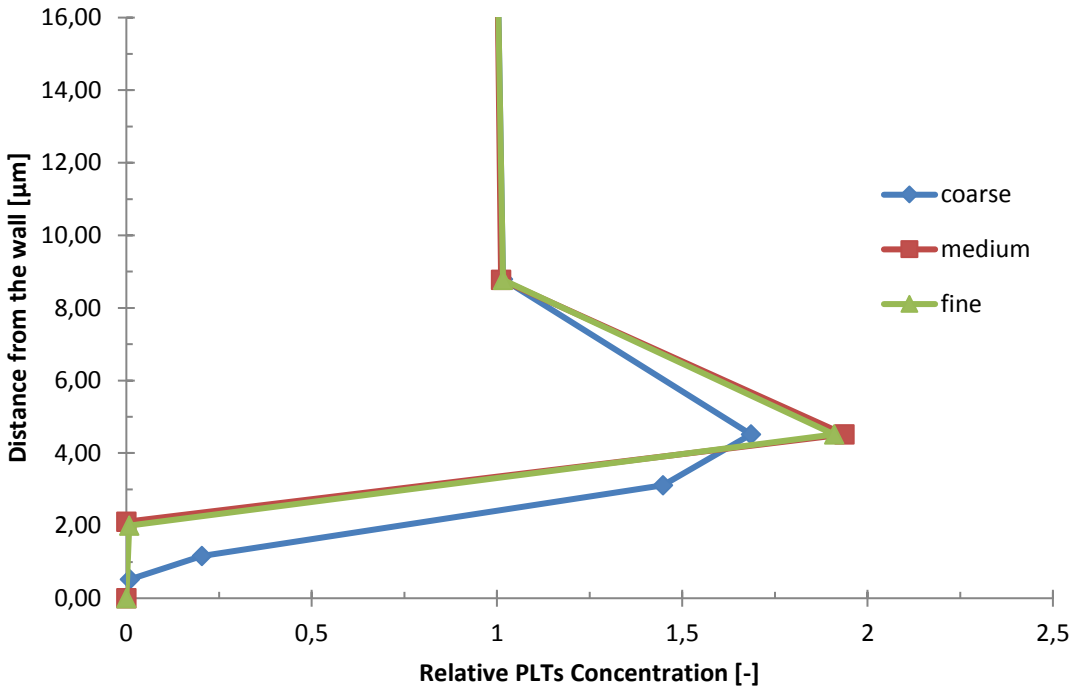

Figure 5. Platelets concentration profile in a section of the tube obtained for 3 different meshes

The relative platelets concentrations of the upper part of the tube for three meshes are shown in Figure 5. As it can be seen, PLT concentration increases as the grid is refined from coarse to medium mesh type, which indicates dependence of the result on cell size. But further refining of the grid from medium to fine mesh presents smaller error in most of the measurement points, indicating oscillatory convergence of the grid. Refinement of the mesh shows the reduction of the apparent order of accuracy range from 14.6 to 0.8%. From these results of the Grid evaluation, medium sized mesh was selected for as the main grid for studies.

4.3.Results and Discussions

The blood cells are modeled as liquid dispersed droplets in a three-dimensional Poiseuille flow, with gravitational acceleration perpendicular to the tube axis, where the Froude number is 0.33. The section of the micro-tube subjected to analysis corresponds to a region of hydrodynamically developed flow far downstream from the inlet at the distance of 70 mm.

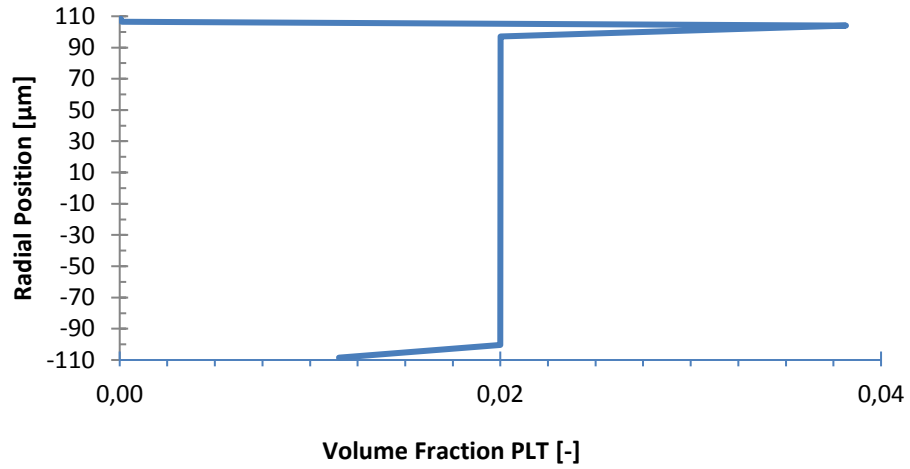

Figure 6. Platelets volume fraction

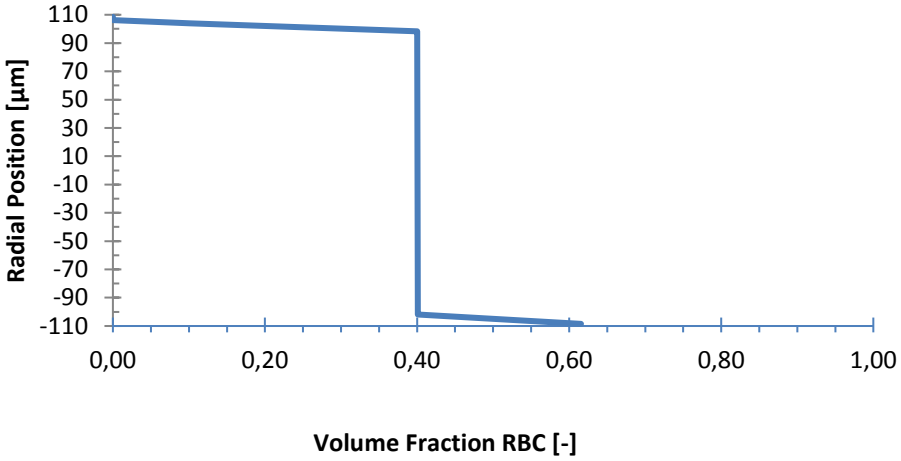

Figure 7.RBC's volume fraction.

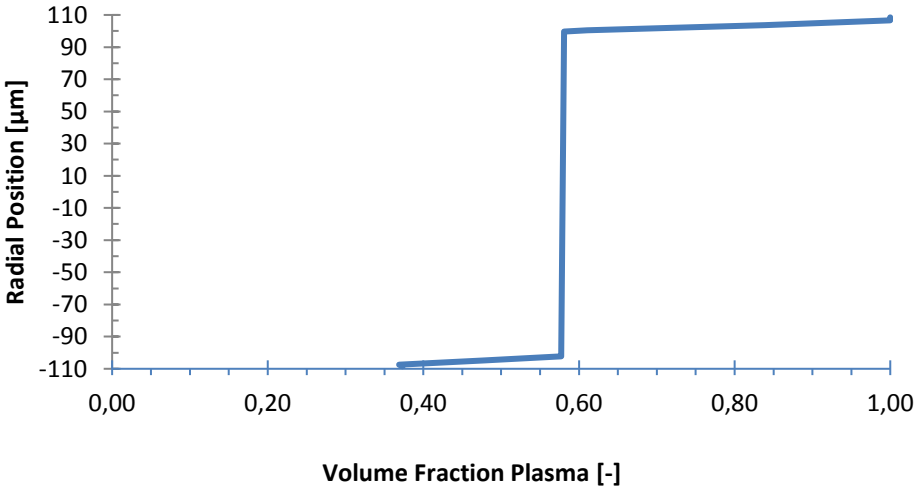

Figure 8. Plasma volume fraction.

Figures 6, 7 and 8 demonstrate volume fraction of the disperse phases and plasma plotted as a function of radial location. RBCs tend to move towards the bottom of the pipe, increasing their concentration in this region, that the result of low Froude number. As they are settled down, a displacement of plasma and platelets occurs towards the upper side of the pipe. On the upper wall plasma has maximum concentration, whereas RBCs has maximum concentration in bottom wall. Generally, this behavior refers to multiphase flow, where the relationship between the channel size and the particle size is relatively large and the Reynolds number is low (Mubita et al., 2014).

The peak in platelets concentration profile (Figure 6) is related to a lateral migration of particles that tend to cluster at a distance from the wall known as the equilibrium position y_e, which is defined as the lateral distance from the centerline of the channel to the peak position of the particle concentration distribution (r/R) (Mubita et al., 2014). Comparing in-vitro results reported by Yeh et al. (1994) and results from multiphase model by Mubita et al. (2014), the equilibrium position for their experimental data is 0.98 and 0.96 respectively, while in the present model, simulation results claim y_e=0.96, similar to Mubita et al. (2014), and with an approximate relative error of 2% with experimental values of Yeh et al. (1994). The relative peak concentration of platelets in this study showed approximate relative error of 0.12% with Mubita et al. (2014) results. Nevertheless, both Multiphase and GKT models demonstrated results approximately 6 times lower than the experimental one.

Model type	Experimental results Yeh et al (1994)	Multiphase model Mubita et al. (2014)	numerical model
Relative Platelets peak concentration	12	1.94	1.937
Equilibrium position y_e	0.98	0.96	0.96

Table 3. Comparison of peak platelets concentration using different models

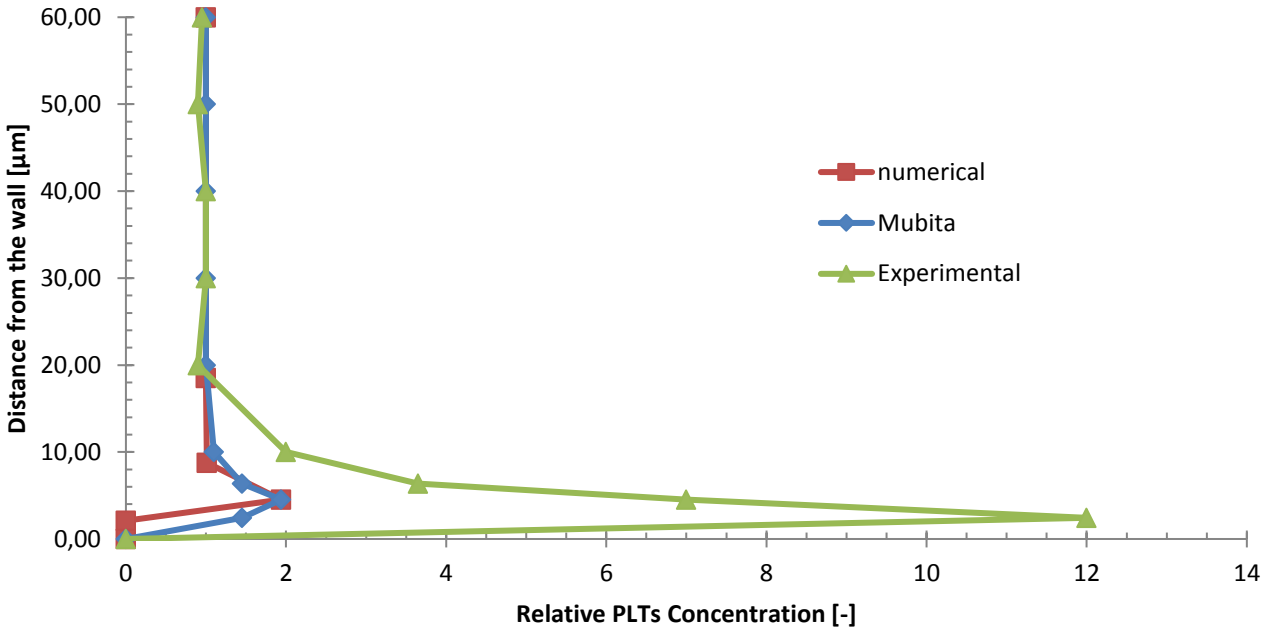

Figure 9. Comparison between the platelets' concentration profile for different methods

To prove that the size of the particles plays an important role in particles migration, the simulations with different hematocrit were compared, in the same manner as it was done by Mubita et al. (2014). PLTs and RBCs are modeled with the same volume fraction (2%) and when they have volume fractions of 2 and 40%, respectively. From the figures 10 and 11 it can be concluded that the peak of highest concentration is still observed for the platelet phase at the same equilibrium position. However, it is placed to the other side of the tube. For RBCs, the concentration profile had no change even though the volume fraction varies from 2 to 40%.

Since the density difference between the plasma and the platelets is small, and the platelet diameters are smaller than the RBC ones, the magnitude of the gravitational force is higher for RBCs and makes the major contribution to the movement of these particles (Mubita et al., 2014).

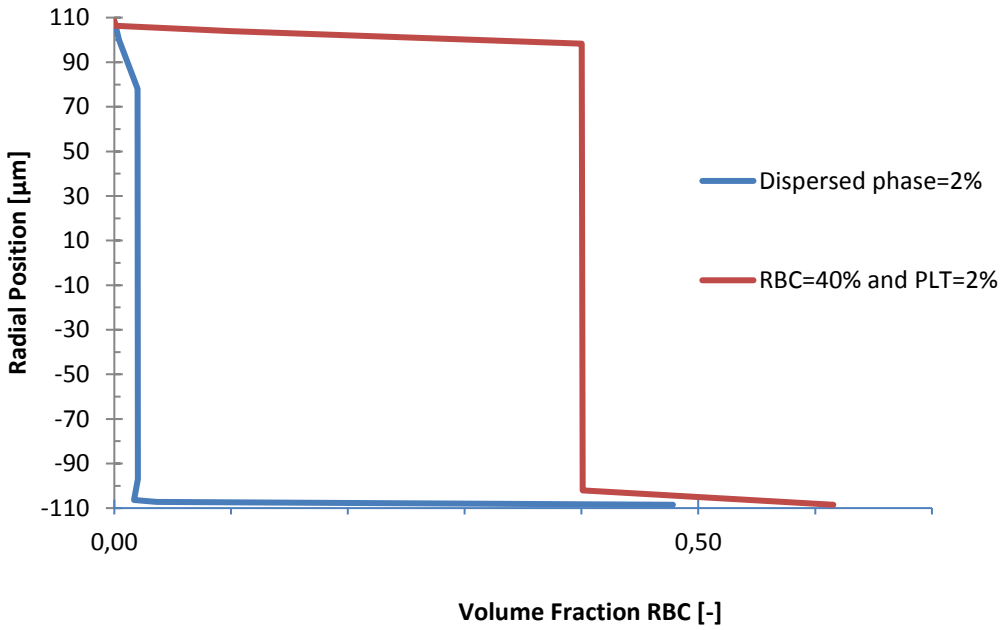

Figure 10. Concentration profile when varying the volume fraction of the dispersed phase at the tube inlet for RBC

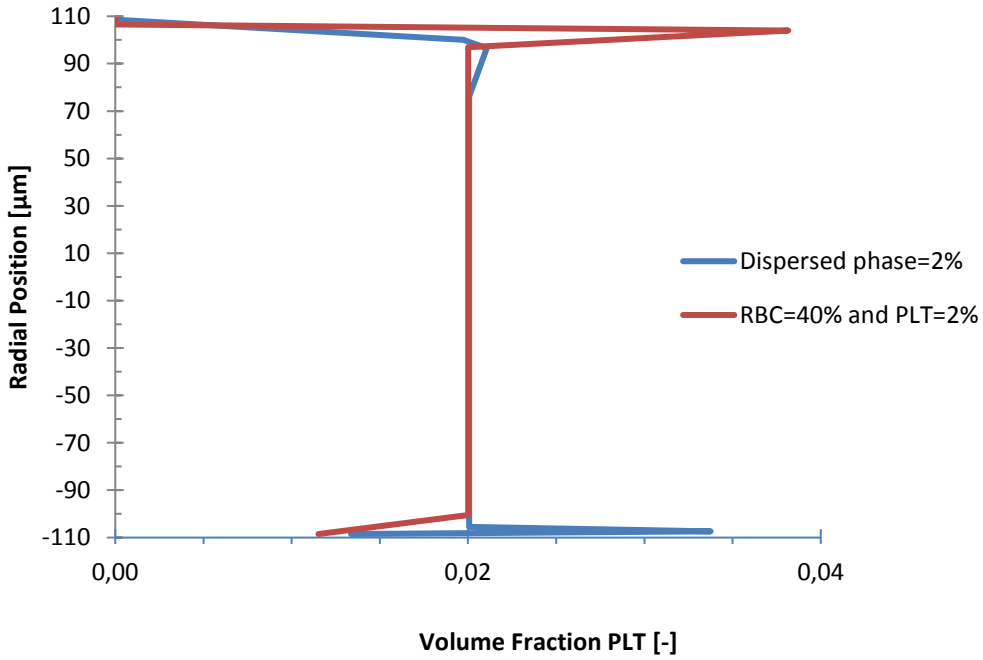

Figure 11. Concentration profile when varying the volume fraction of the dispersed phase at the tube inlet for PLT

4.4.Evaluation of input parameters on final results

This section will present the results of the analysis on how the F-L effect is predicted under variation of input parameters that affect the particles migration within the flow. Following were the empirical inputs in the model used for the analysis: Packing Limit, Restitution coefficient, Sauter mean diameter and Drag coefficient between solid phases and liquid.

4.4.1. Packing Limit

At equilibrium RBCs tend to have a biconcave shape that corresponds to a minimal membrane bending energy (Figure 12), while platelets show biconvex discoid (lens-shaped) structures (Kaoui et al., 2009). Under non-equilibrium conditions, as experienced in a simple shear flow, RBCs reveal number of different shapes and dynamics. Platelets shape also continuously changes from the inactivated to the fully activated state, which their shape irregularities should be taken into account in the modeling process. Nevertheless, inexpensive CFD tools such as ANSYS Fluent are not powerful enough to capture such shape irregularities of the particles. Therefore, RBC and platelets were assumed to be rigid spherical particles, which is very rough approximation. However, there are several parameters we are able to explore in order to take into account the non-spherical shape of those particles. The one such input parameter is the Packing limit, which is an empirical parameter used to characterize the maximum volume fraction of solid objects obtained when they are packed randomly (Torquato et al., 2000). For the spherical shape particles, the packing limit is around 0.63, and the greater deviation from the spherical shape of RBCs, the denser is the packing. To take into account the deviation of RBC and platelets from the sphere shape, peak platelets concentration for RBC and platelets was studied against the Packing limit value. Before, the simulations with different Packing limits were conducted, we hypothesized that with an increase of the Packing limit peak concentration of platelet particles in the top part of the channel will increase, as less platelets will be able to accumulate between larger particles, RBC, because their Packing limit will increase too, and thus will lead to more segregation of the platelets from the centerline. Numerical simulations with Packing limit smaller than 0.5 were not fully converged, therefore the total range of the Packing limit presented were in the range from 0.5 to 1.0.

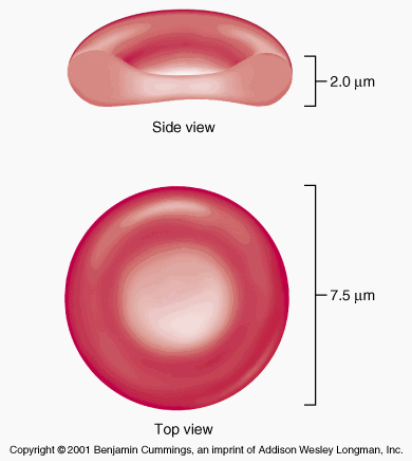

Figure 12. Red blood cells shape (source: Morphological Abnormalities of Red Blood Cells, 2015.)

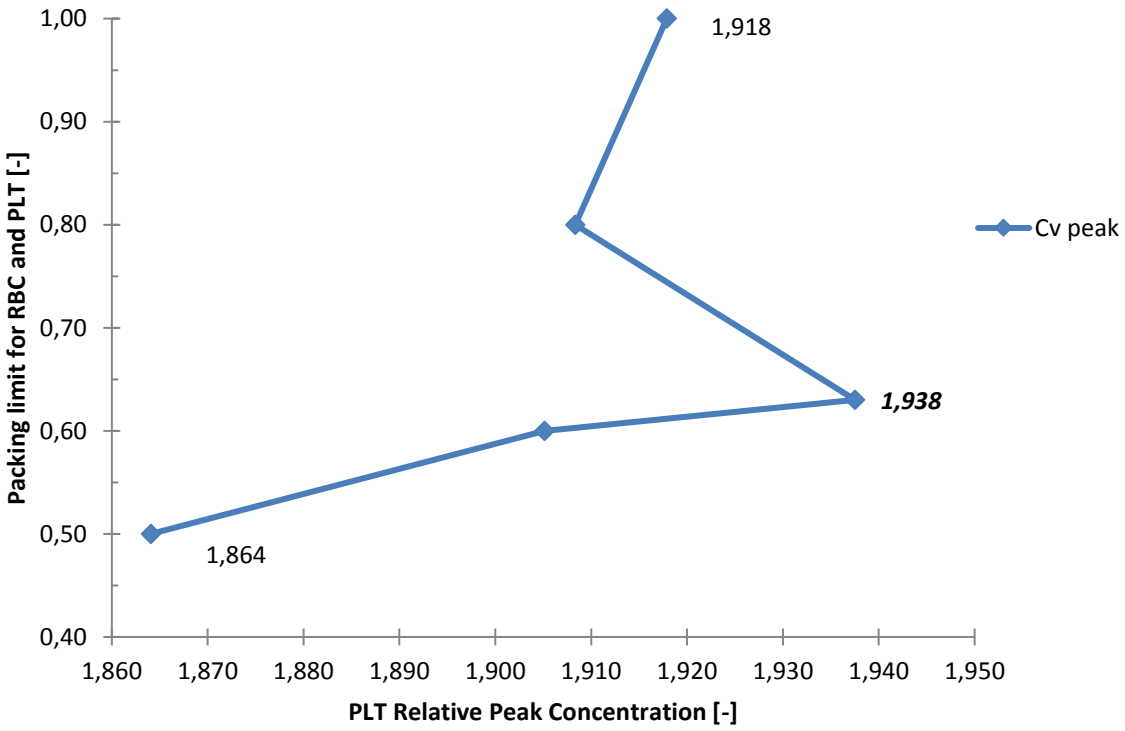

Figure 13. Dependency of Packing limit of particles on Relative PLT concentration

As it can be observed from the Figure 13, relative peak of the platelets concentration shows non-linear correspondance with changing of packing limit for both RBC and platelet particles from default value for sphereical shape of 0.63. The hypothesis that by increasing

packing limit the particles shape would be assumed to have less spherical properties and thus produce results closer to experimental values wasn't proven. Nevertheless, the maximum relative error for peak concentration is around 1.5%, thus producing negligible difference. Therefore we can conclude that the packing limit doesn't play a prominent role in particles segregation simulated on CFD tool.

4.4.2. Restitution Coefficient

The restitution coefficient, *e*, is a measure of the elasticity of the particle collisions. It is defined as the ratio of rebound velocity of particle to its velocity before impact. In the present study, RBC and platelets were assumed to be rigid spherical particles, whereas they have rather complex structure in the real conditions. To include the deformability of these particles, restitution coefficients were adjusted to account for their deviation of shape from ideal sphere. In Gidaspow (2009), the *e*=0.95 was chosen between RBC particles and e_w=0.60 between RBC particles and the wall. For simplicity of the model, the restitution coefficient in collisions between similar and distinct particles, as well as in collisions between particles and the wall, was changed simultaneously and for the same value. By lowering the restitution coefficient we assume energy more dissipation after each collision. We hypothesized that with increasing restitution coefficient above the standard value of e=0.95, segregation will be more prominent and thus, higher platelets peak concentration will be observed. On the other side, by lowering *e* value we also expect higher platelets clustering at the walls as the dominance of inelastic collision could lead to greater role of gravitational forces, which is also a major reason for RBC segregation.

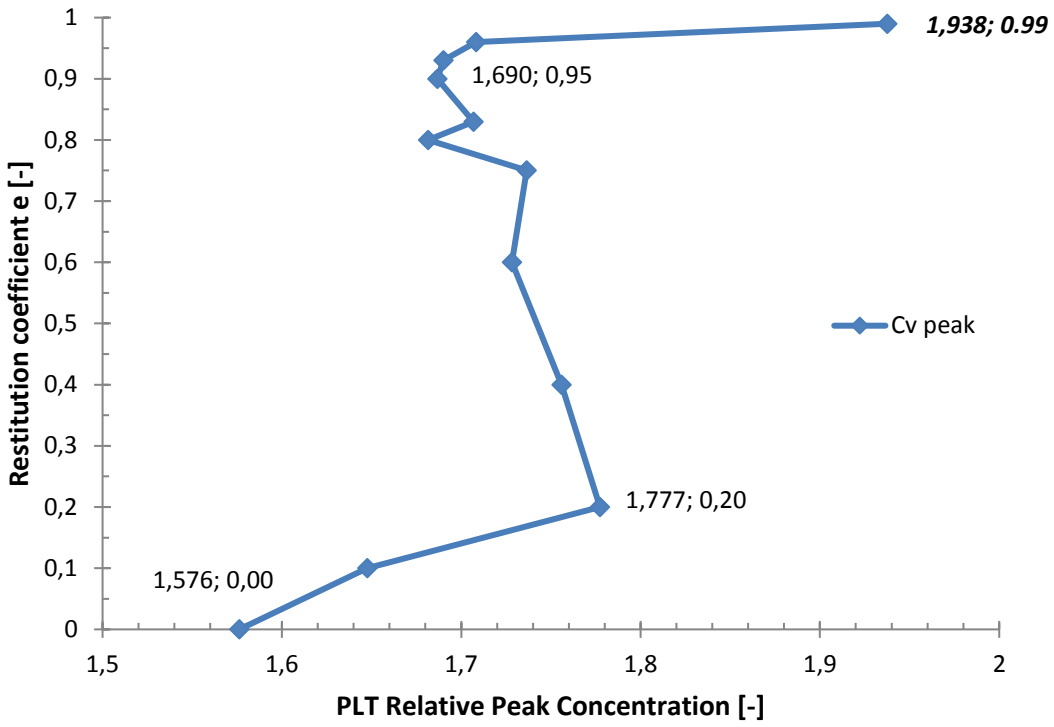

Figure 14. Dependency of restitution coefficients on Relative PLT concentration

As it can be seen from the Figure 14, our assumptions were partially true. By increasing restitution coefficient from 0.95 to 0.99 led to an increase of platelets peak concentration from 1.690 to 1.938, an increase of almost 15%. Also, by lowering *e* to the value of 0.2, less prominent increase in peak can be seen (an increase of 5%). However, by reducing the restitution coefficient e<0.2, the platelets clustering was gradually decreased reaching 1.576 relative concentration for completely inelastic particle-particle and particle-wall collisions.

4.4.3. Sauter mean diameter of particles

As it was previously mentioned, RBC and platelets do not have specific shape as their shape continuously change in the course of the flow. However, as CFD tools have limitation for particles shape, all particles are assumed to have spherical shape with specific Sauter mean diameters, which is an average of particle size. For this study, Sauter mean diameters of 6μm for RBCs and 2.5 μm for PLTs are assumed, provided from the Mubita et al. (2014). Nevertheless, these values are only assumptions made by the authors and the real values can vary for each

individual, from healthy to ill person. In this section, the effect of Sauter mean diameter of RBC and platelets on the peak platelets concentration in the blood flow will be observed. For RBC, the range was from 3 μm to 8 μm, while for platelets from 1.25 μm to 3.75 μm, as simulations with greater and lower values were not fully converged and are not in the physical range of human blood particles.

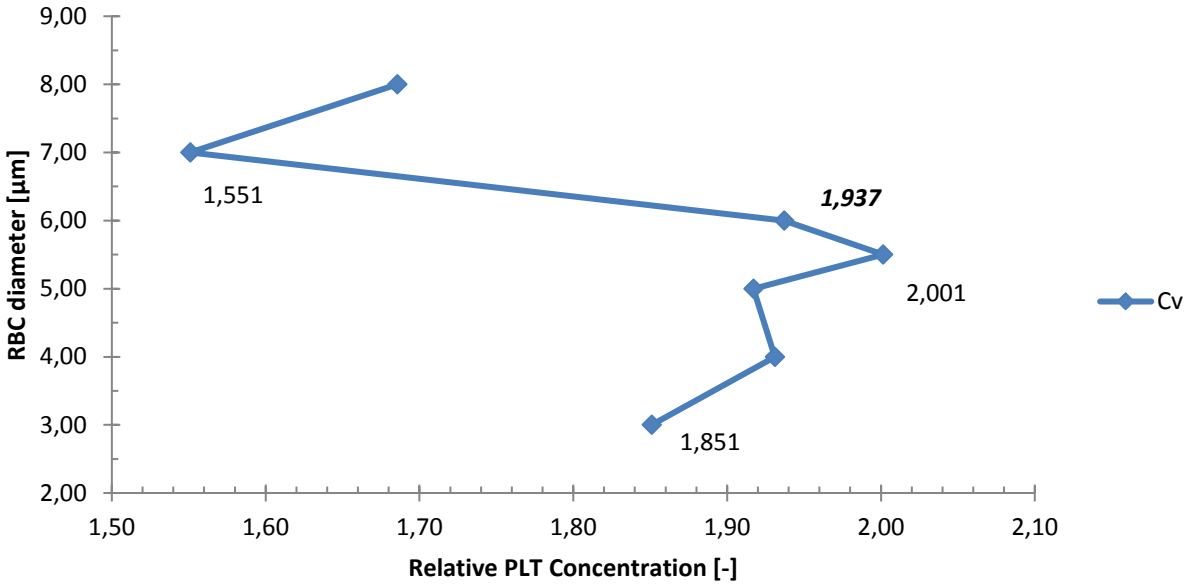

Figure 15. Dependency of RBC diameter on Relative PLT Concentration

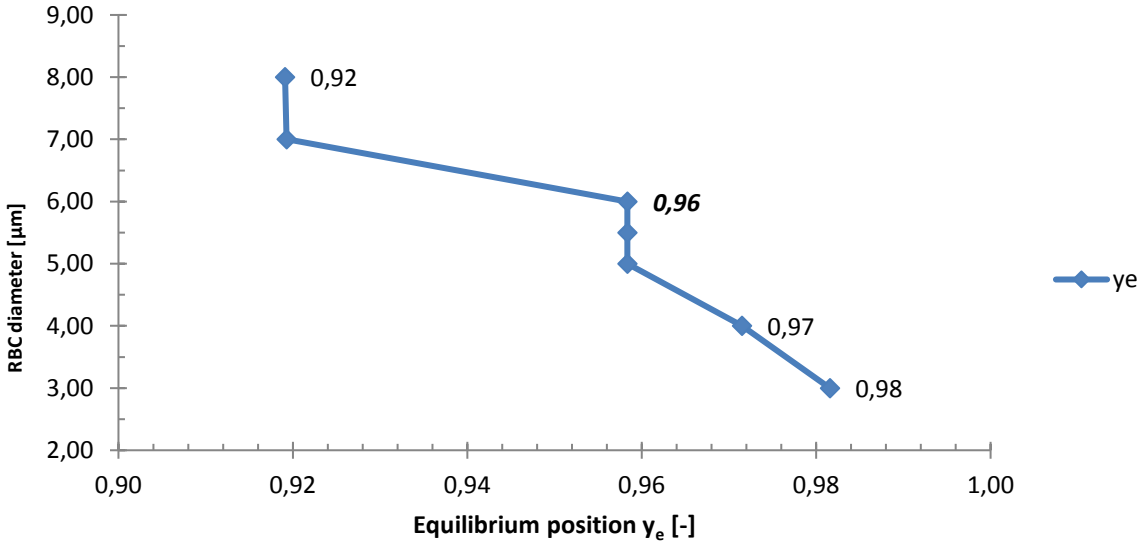

Figure 16. Dependency of RBC diameter on equilibrium position y_e

From the figure 15 it can be observed that the change in Sauter mean diameter of the RBC from the original value of 6 μm produces nonlinear dependency with maximum platelets concentration in the upper part of the microtube. The minimum relative peak of 1.551 can be seen for the diameter of 7 μm while the maximum peak volume fraction is observed for the diameter of 5.5 μm. For the diameters lower than 5.5 μm the gradual reduction in relative concentration is monitored.

On the figure 16, we can observe dependency of RBC size on an equilibrium position y_e. Interestingly that by reducing Sauter mean diameter of RBC leads to closer clustering of platelets to the wall area. If mean diameters from 5-6 μm produce equilibrium position of 0.96, similar to numerical results by Mubita et al. (2014), smaller diameter of 3 μm makes platelets to cluster at an equilibrium position of y_e=0.98, which is closer to in-vitro results by Yeh et al (1994).

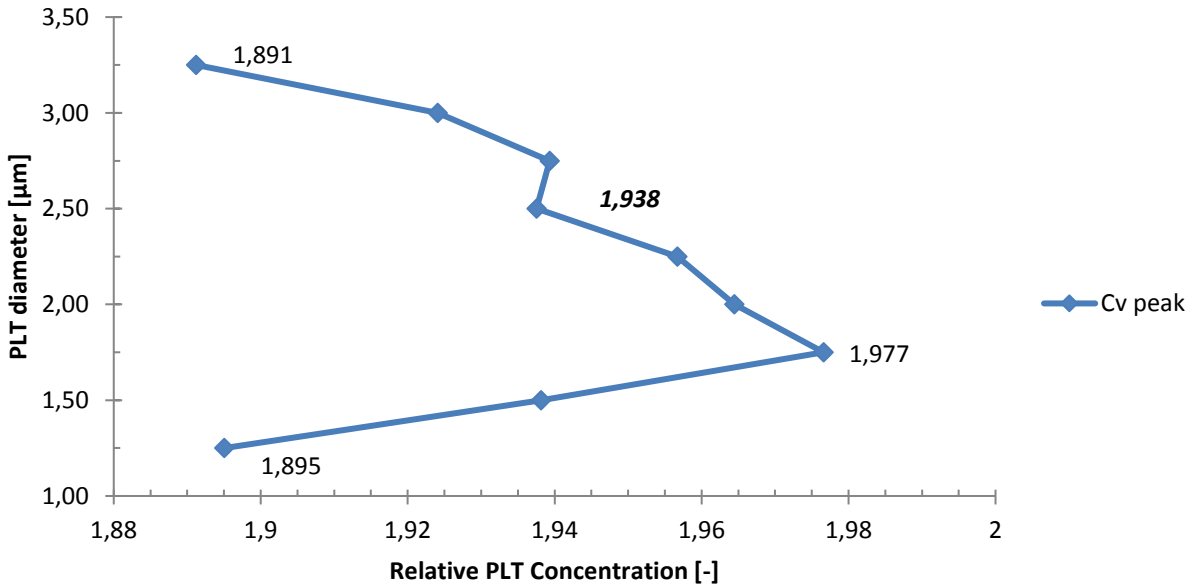

Figure 17. Dependency of PLT diameter on Relative PLT Concentration

Figure 17 represents Dependency of PLT diameter on Relative PLT Concentration, which indicates that the platelets with Sauter mean diameter of 1.75 mm shows the highest platelets peak concentration of 1.977. It is observed that by altering of the diameter from this value results in gradual reduction of the platelets volume fraction. Nevertheless, the difference between the lowest and highest values gives relative error of 4.5%. Therefore, we can summarize that the

variation of platelets Sauter mean diameter doesn't have prominent effect on the particles segregation.

4.4.4. Drag Coefficient

In this section, the effect of drag between dilute phases and plasma will be discussed. For all simulation Gidaspow drag model was used for particle-liquid as well as particle-particle interaction, as this model is suitable for dense fluidized bed applications, as it is our case.

4.4.4.1.Drag between RBC and plasma

As it was mentioned before, due to the non-spherical shapes of the blood particles it is difficult to predict appropriate drag coefficient for the particle-liquid interactions, as the difference in shapes between real-life particles and the particles that are assumed to have rigid spherical shape can be great. To understand the importance of drag force between plasma and RBC on the segregation process, series of simulation were produced to find their correlation. We hypothesized that with an increase of the drag coefficient the platelets clustering will reduce as an increased drag between plasma and RBC will lead to more active entraining of the latter along the flow main stream, thus preventing RBC segregation.

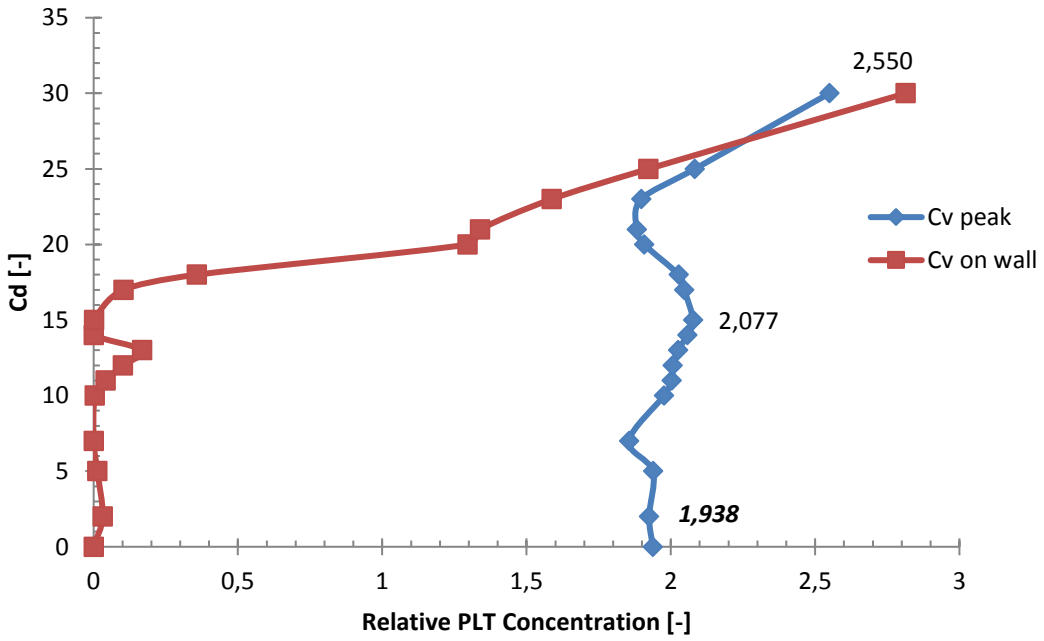

Figure 18. Dependency of Cd between Plasma and RBC on Relative PLT concentration

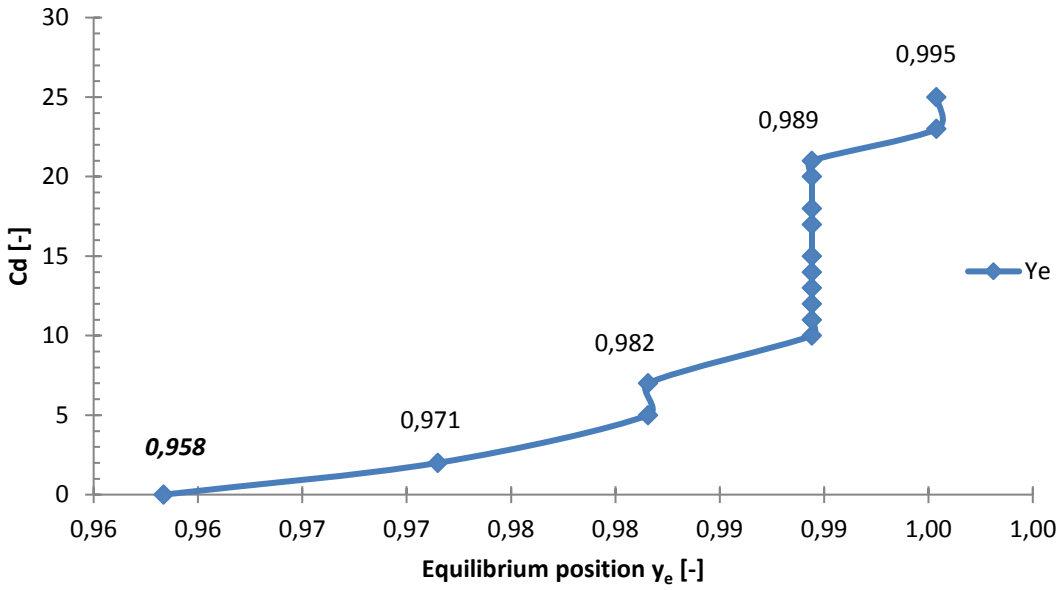

Figure 19. Dependency of Cd between Plasma and RBC on equilibrium position y_e

As it can be observed from the Figure 18, peak relative platelets concentration reaches the maximum value of 2.077 at Cd=15. Because of the repulsion forces platelets cannot go all the way onto the wall, so they will accumulate at a stand-off distance from one of the walls. The red line of the Figure 18 shows the value of relative platelets concentration immediately to the wall, which is almost 0 for Cd<15. But as the drag between RBC and plasma increases, the platelets start to accumulate right on the wall region. Rising Cd to a value of Cd=27, eventually leads red line to surpass the blue one, thus platelets concentration immediately on the wall will be the highest over the entire profile, thus shifting a peak right on the wall region. This behavior can be confirmed on Figure 19, where the rising of equilibrium position can be observed till Cd=27, when y_e eventually become equal to 1.

4.4.4.2.Drag between PLT and plasma

As for the drag between plasma and platelet particles, we expect the same effect as with RBC. An increased drag between particle and fluid will lead to more prominent particle entrainment along the flow main stream, thus preventing clustering.

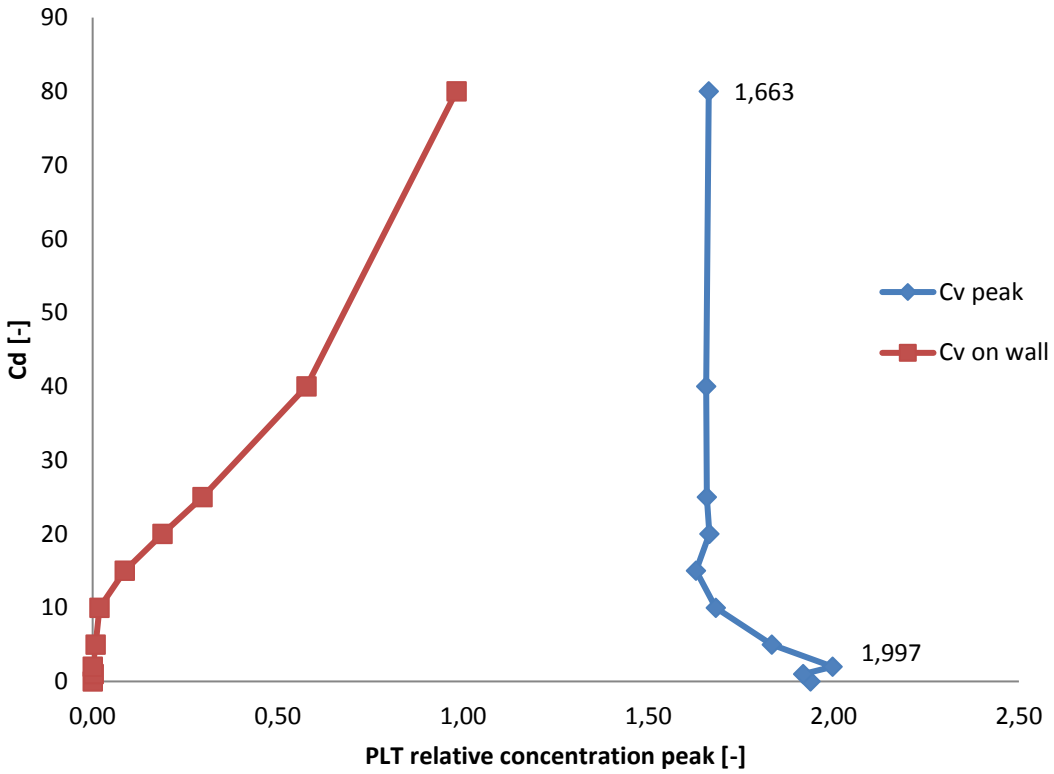

Figure 20. Dependency of Cd between Plasma and PLT on Relative PLT concentration

As it can be observed from Figure 20, increasing the drag coefficient produce a slight increase of 1.997 relative platelets concentration at Cd=2, but with further increase of Cd, concentration drops to the value of around 1.663 and remains constant until Cd=80. Platelets began to cluster immediately the wall starting from Cd=2 and gradually rising until Cd=80. Simulations with drag coefficients greater than Cd>80 are assumed unrealistic for flow conditions in microtube, therefore further simulation were not included in the study.

5. Conclusion

This capstone project has presented results of an attempt to improve and validate a numerical CFD model to accurately predict blood trauma within medical blood-wetted devices. The key difference of the present model from other authors was in the incorporation of the Granular Kinetic Theory which was expected to capture a more realistic cell-cell interaction, cell-wall and cell-plasma interaction such that the prediction of the Fahraeus-Lindqvist effect is improved and therefore a better damage modeling might be obtained in the next stage of the calculation. In the implementation phase we came to a conclusion that the implementation of GKT improved the model as it took into account not only interactions between disperse and continuum phases, but also the interactions among the disperse phases. Nonetheless, the difference in platelets segregation between GKT model proposed in the paper and the multiphase model by Mubita et al. (2014) was not prominent and claimed only small improvements. To analyze the possible reasons for model's results discrepancy the capstone team selected several simulation parameters for in-depth analysis on how the Fahraeus-Lindqvist effect is predicted under variation of parameters that affect the particles segregation within the flow. During the analysis study, modification of none of the input parameters didn't significantly affect an increase of platelets clustering, though some of the parameters should be taken into account for future work.

Initial objectives of the project included the improvement, validation, incorporation of damage and optimization of the cannula tip for medical devices. Nevertheless, due to time limitations and complexity of the problem capstone team decided to re-dimension the scope of the project to the improvement of the F-L effect as a mean to grant a better base model to further predict later blood damage and subsequent optimization of the cannula or other blood-wetted devices. Therefore, possible objectives for the future work would be the incorporation of the damage model and optimization of the cannula tip with the use of GKT.

Reference:

1. Davletov, Kairat, et al. "Age-specific mortality analysis helps to explain all-cause mortality decline in Kazakhstan." The European Journal of Public Health 25, suppl 3 (2015): ckv176-303.
2. Eckstein, Eugene C., and Fethi Belgacem. "Model of platelet transport in flowing blood with drift and diffusion terms." Biophysical journal 60.1 (1991): 53-69.
3. Fahraeus, Robin, and Torsten Lindqvist. "The viscosity of the blood in narrow capillary tubes." American Journal of Physiology--Legacy Content 96.3 (1931): 562-568.
4. Gidaspow, Dimitri, and Jing Huang. "Kinetic theory based model for blood flow and its viscosity." Annals of biomedical engineering 37.8 (2009): 1534-1545.
5. Giersiepen, M., et al. "Estimation of shear stress-related blood damage in heart valve prostheses--in vitro comparison of 25 aortic valves." The International journal of artificial organs 13.5 (1990): 300-306.
6. Gonzalez, J., L. Rojas-Solorzano, and N. Sabirgalieva. "Numerical simulation of slurry flows in heterogeneous and saltation regimes in horizontal pipelines." (2014).
7. Kaoui, Badr, George Biros, and Chaouqi Misbah. "Why do red blood cells have asymmetric shapes even in a symmetric flow?" Physical review letters 103.18 (2009): 188101.
8. Kulkayeva, Gulnara, et al. "Cardiovascular disease risk factors among rural Kazakh population." Nagoya journal of medical science 74.1-2 (2012): 51.
9. Maton, Anthea; Jean Hopkins, Charles William McLaughlin, Susan Johnson, MaryannaQuon Warner, David LaHart, Jill D. Wright (1993). Human Biology and Health. Englewood Cliffs, New Jersey: Prentice Hall. ISBN 0-13-981176-1.
10. “Morphological Abnormalities of Red Blood Cells.” WordPress, 5 Sept. 2015, https://theartofmed.wordpress.com/2015/09/05/morphological-abnormalities-of-red-blood-cells/
11. Mubita, T. M., L. R. Rojas-Solórzano, and J. B. Moreno. "A Multiphase Approach to Model Blood Flow in Micro-tubes." Computational and Experimental Fluid Mechanics with Applications to Physics, Engineering and the Environment. Springer International Publishing, 2014. 235-247.

12. Mubita, T. M., L. R. Rojas-Solórzano, Mansur Zhussupbekov and Lyazzat Zhanshayeva. “CFD Modeling of Hemolysis in Medical Devices used in the Treatment of Cardiovascular Disease (CVD).” (2015)
13. Pya, Yuriy, et al. "Initial 3-year outcomes with left ventricular assist devices in a country with a nascent heart transplantation program." ESC heart failure 3.1 (2016): 26-34.
14. Salazar, Félix A., Luis R. Rojas-Solórzano, and Armando J. Blanco. "Turbulence modeling in the numerical estimation of hemolysis in hemodialysis cannulae." Revista de la Facultad de Ingenieria UCV 23.4 (2008): 93-98
15. Stewart, Sandy FC, et al. "Preliminary results of FDA’s ‘Critical Path’ project to validate computational fluid dynamic methods used in medical device evaluation." ASAIO J 55.2 (2009): 173.
16. Tandon, Elias and Lo. “Comparative analysis of two multiphase modelling approaches for blood flow.” Eleventh International Conference on CFD in the Minerals and Process Industries. CSIRO, Melbourne, Australia (2015)
17. Tandon, Pushkar, and Scott L. Diamond. "Hydrodynamic effects and receptor interactions of platelets and their aggregates in linear shear flow." Biophysical journal 73.5 (1997): 2819-2835.
18. Torquato, Salvatore, Thomas M. Truskett, and Pablo G. Debenedetti. "Is random close packing of spheres well defined?." Physical review letters 84.10 (2000): 2064.
19. Waldenberger, F. R. "Pathophysiological considerations concerning uni and biventricular mechanical cardiac assist." The International journal of artificial organs 20.12 (1997): 684-691.
20. World Health Organization. World health statistics 2010. World Health Organization, 2010.
21. World Health Organization. World health statistics 2011. World Health Organization, 2011.
22. Yeh, Chinjung, Anne C. Calvez, and Eugene C. Eckstein. "An estimated shape function for drift in a platelet-transport model." Biophysical journal 67.3 (1994): 1252-1259.
23. Zhao, Rui, et al. "Micro-flow visualization of red blood cell-enhanced platelet concentration at sudden expansion." Annals of biomedical engineering 36.7 (2008): 1130.